

Development of a magnetic resonance microscope using a high T_c bulk superconducting magnet

Kyohei Ogawa,¹ Takashi Nakamura,² Yasuhiko Terada,¹ Katsumi Kose,^{1,a)} and Tomoyuki Haishi³

¹Institute of Applied Physics, University of Tsukuba, Tsukuba 305-8573, Japan

²RIKEN, Wako 351-0198, Japan

³MRTechnology, Tsukuba 305-0047, Japan

(Received 16 March 2011; accepted 16 May 2011; published online 9 June 2011)

We have developed the first magnetic resonance (MR) microscope using a high critical-temperature superconducting bulk magnet. The bulk magnet comprises six annular bulk superconductors (60 mm outer diameter, 28 mm inner diameter, 20 mm high) made of c-axis oriented single-domain $\text{EuBa}_2\text{Cu}_3\text{O}_y$ crystals. The magnet was energized using a superconducting NMR magnet operating at 4.7 T. The inhomogeneity of the trapped magnetic field measured with MR imaging was 3.1 ppm (rms) in the $\phi 6.2 \text{ mm} \times 9.1 \text{ mm}$ cylindrical region. Three-dimensional MR images of a chemically fixed mouse embryo acquired with voxels of $(50 \mu\text{m})^3$ demonstrated the potential of our system. © 2011 American Institute of Physics. [doi:10.1063/1.3598440]

The magnetic resonance (MR) microscope is a magnetic resonance imaging (MRI) system that achieves a spatial resolution of $<100 \mu\text{m}$ for small animals and intact specimens.¹⁻³ Until now, MR microscopes have been constructed using superconducting⁴ and permanent magnets.⁵ These have both advantages and disadvantages. Superconducting magnets for MR microscopes provide high and very stable magnetic fields (up to about 19 T),⁴ but require large installation spaces and cryogen refill (liquid He and N_2). Permanent magnets for such instruments require neither cryogen nor large installation spaces, but the field strength is limited up to about 2 T.⁶

In 2007, a novel magnet for nuclear magnetic resonance (NMR) using a high critical-temperature (T_c) superconducting (HTS) bulk material was reported by Nakamura *et al.*⁷ This magnet has overcome the above disadvantages in MR microscope magnets as it provides a high and stable magnetic field, but requires neither cryogen refill nor a large installation space. In this study, we developed the first MR microscope using a HTS bulk magnet and evaluated its possibility for small animal MRI systems.

Figure 1 shows an overview of the MR microscope. The system consists of a superconducting bulk magnet, a gradient coil set, a radio frequency (rf) probe, and an MRI console. As shown in Fig. 2, the bulk magnet comprised vertically stacked six annular bulk superconductors (outer diameter = 60 mm, inner diameter = 28 mm, height = 20 mm) made of c-axis oriented single-domain $\text{EuBa}_2\text{Cu}_3\text{O}_y$ crystals with a superconducting transition temperature of 93 K.⁸ The bore size and the vertical height of the annular bulk magnets were carefully determined using a finite element method calculation to obtain a homogeneous magnetic field around the center of the magnet. The bulk superconductors were reinforced to protect them from break caused by the huge electromagnetic hoop stress during the field cooling process using aluminum rings (thickness = 5 mm), stored in a cryostat (outer diameter = 88 mm, room temperature bore diameter

= 20 mm) made of Al alloy, and cooled using a pulse tube refrigerator.

The gradient coil set was wound on an acrylic pipe (outer diameter = 16.8 mm, inner diameter = 14.8 mm) using 0.3 mm diameter polyurethane-coated Cu wire. The axial gradient coil was a Maxwell pair coil and the transverse gradient coils were Golay coils. Efficiencies of the G_x , G_y , and G_z coils were 81 mT/m/A, 93 mT/m/A, and 106 mT/m/A, respectively. The rf coil was a single-turn saddle-shaped coil wound on an acrylic pipe (outer diameter = 12 mm, inner diameter = 9 mm) using 0.1-mm-thick Cu foil. The rf probe was tuned to 200.0 MHz using two variable capacitors and one fixed. A cylindrical rf shield made of 0.1-mm-thick Cu foil was inserted between the gradient and the rf coils to block any rf coupling between them. The gradient set and the rf probe were inserted into the room temperature bore of the bulk magnet and connected to the MRI console (MRTechnology, Tsukuba, Japan).

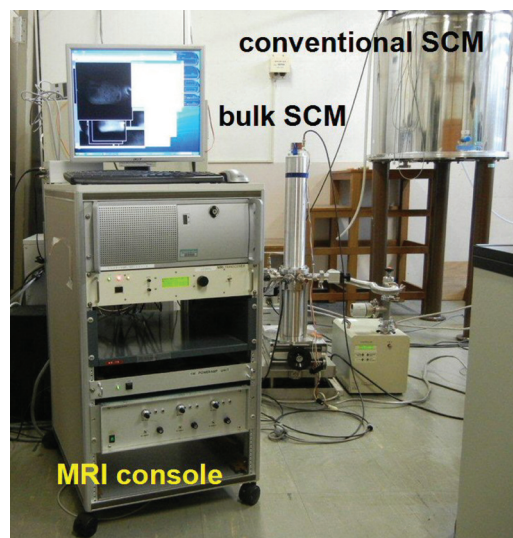


FIG. 1. (Color) The MR microscope developed in this study. The superconducting bulk magnet is seen in the center of the figure. The conventional superconducting NMR magnet used for energizing the bulk magnet is seen behind the bulk magnet.

^{a)}Electronic mail: kose@bk.tsukuba.ac.jp.

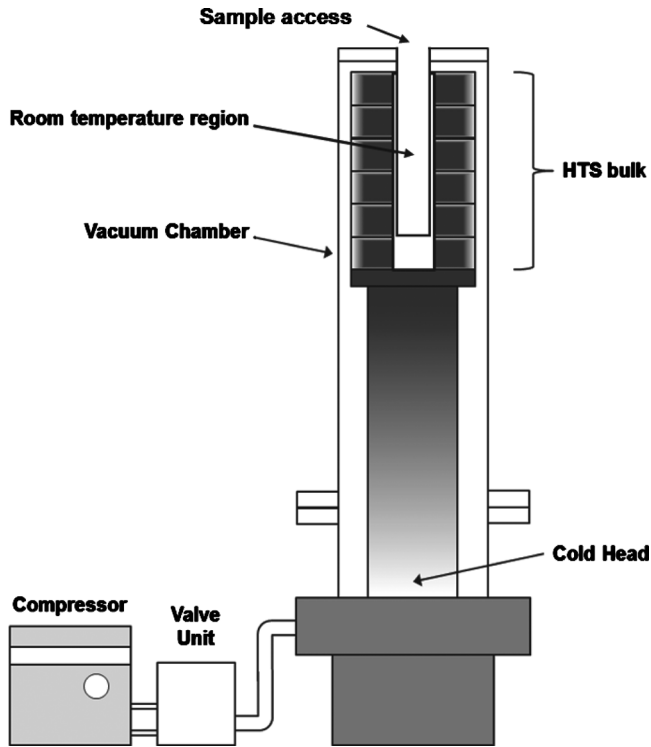


FIG. 2. Schematic of the HTS bulk magnet.

The bulk magnet was energized as follows.^{7,9} The temperature of the magnet was kept above the T_c (about 100 K) of the superconductor, and the bulk magnet was inserted into the room temperature bore of a conventional superconducting NMR magnet (JMTC-300/89, JASTEC, Kobe, Japan) generating a 4.7 T homogeneous magnetic field. The bulk material was cooled down to 50 K under the homogeneous magnetic field with superconducting shimming, and the electrical currents of the main magnet and shim coils were decreased slowly to zero. Magnetic flux generated by the superconducting magnet was trapped by the bulk superconductor and a homogeneous magnetic field of 4.7 T was produced in the bore of the bulk magnet. In this situation, a superconducting current distribution was present in the bulk material. From 10 days after the energizing of the bulk magnet, we measured the magnetic field drift for two weeks. The drift was very small and almost constant ($\sim +0.018 \mu\text{T/h}$).

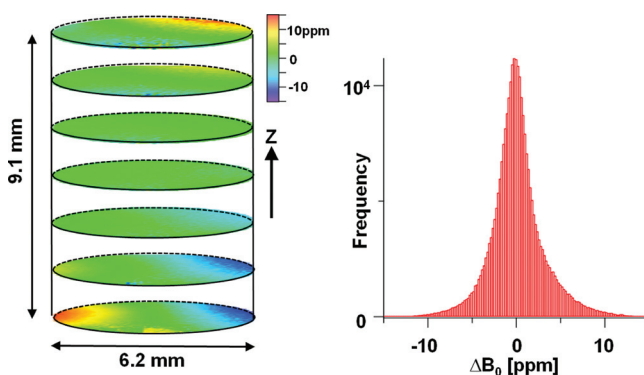


FIG. 3. (Color) Magnetic field distribution (left) and its histogram (right) measured in the central $\phi 6.2\text{mm} \times 9.1$ mm region of the bulk magnet. Root mean square and peak-to-peak values of inhomogeneity were 3.1 ppm and 37 ppm, respectively.

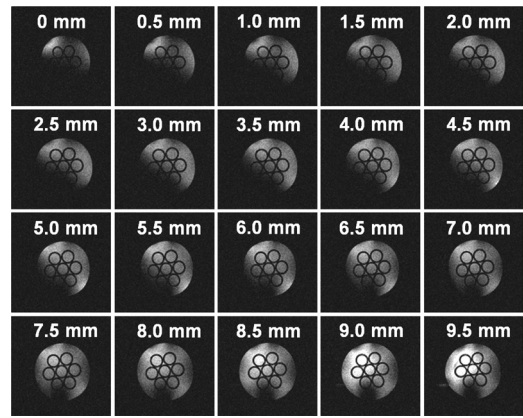


FIG. 4. 2D cross sections selected from a 3D image data set of a water capillary phantom. Numbers in the images are the vertical heights of the images. The voxel size is $(100 \mu\text{m})^3$.

The spatial distribution of the magnetic field in the bore of the bulk magnet was measured in the central $\phi 7.0\text{mm} \times 12.8$ mm cylindrical region using a conventional phase-shift method and NiSO_4 -doped water in an 8-mm-diameter NMR sample tube. A water phantom with seven capillaries and a chemically fixed mouse embryo (Jcl:ICR strain, 14 days postconception) stored in NiSO_4 -doped water were measured using three-dimensional (3D) spin-echo sequences to evaluate the performance of the MR microscope.

Figure 3 shows the spatial distribution and a histogram of the magnetic field measured in the $\phi 6.2\text{mm} \times 9.1$ mm cylindrical region. Peak-to-peak and root mean square values of the inhomogeneity were 37 ppm and 3.1 ppm, respectively. Figure 4 shows two-dimensional (2D) cross sections selected from a 3D image data set of the capillary phantom acquired with a 3D spin-echo sequence [TR(repetition time)/TE(echo time)=100 ms/10 ms, image matrix= 128^3 , voxel size= $(100 \mu\text{m})^3$, NEX(number of excitation)=1]. Although signal voids caused by a considerable offset of the magnetic field and inhomogeneity of the rf field are evident in the images, the detailed structure of the phantom is visualized clearly.

Figure 5 shows midsagittal and horizontal cross sections of the mouse embryo selected from a 3D image data set acquired with a 3D spin-echo sequence [TR/TE=100 ms/10 ms, image matrix= $128 \times 128 \times 256$, voxel size= $(50 \mu\text{m})^3$, NEX=32]. Although background signal from the NiSO_4 solution is present, the internal structures of the embryo are visualized clearly. These images also demonstrate that no detectable magnetic field drift was present during data acquisition (14.5 h).

From the above experiments, although previous studies¹⁰⁻¹² could not make homogeneous magnetic field suitable for MRI or MR microscopy, we have demonstrated that the temporal stability and spatial homogeneity of the magnetic field produced by our bulk magnet are sufficient for MR microscopy of small samples. The available volume for MR imaging is currently smaller than that of conventional superconducting magnets, but the bulk magnet is cryogen free and compact, which is advantageous over conventional superconducting magnets. If we require a larger volume for small animal MRI using bulk magnets, larger HTS bulk crystals¹³ and an advanced field shimming technique¹⁴ will be required. In conclusion, we have developed the first MR

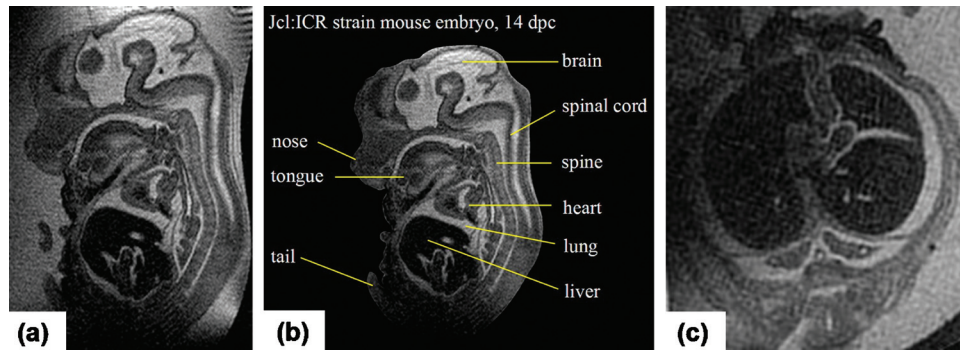


FIG. 5. (Color) The midsagittal [(a) and (b)] and horizontal (c) cross sections of mouse embryo chemically fixed at 14 days postconception (dpc) measured using the MR microscope. The voxel size is $(50 \mu\text{m})^3$. The background signal was manually removed for clarity in (b).

microscope that uses a superconducting bulk magnet and have shown the potential of our system.

¹P. Callaghan, *Principles of Nuclear Magnetic Resonance Microscopy* (Oxford University Press, Clarendon, 1991).

²*Magnetic Resonance Microscopy*, edited by B. Blümich and W. Kuhn (VCH, Weinheim, 1992).

³P. Glover and P. Mansfield, *Rep. Prog. Phys.* **65**, 1489 (2002).

⁴M. Weiger, D. Schmidig, S. Denoth, C. Massin, F. Vincent, M. Schenkel, and M. Fey, *Concepts Magn. Reson., Part B* **33B**, 84 (2008).

⁵T. Haishi, T. Uematsu, Y. Matsuda, and K. Kose, *Magn. Reson. Imaging* **19**, 875 (2001).

⁶T. Haishi, M. Aoki, and E. Sugiyama, *Proc. Int. Soc. Mag. Reson. Med.* **13**, 869 (2005).

⁷T. Nakamura, M. Yoshikawa, Y. Itoh, and H. Koshino, *Concepts Magn.*

Reson., Part B **31B**, 65 (2007).

⁸S. Nariki, N. Sakai, I. Hirabayashi, M. Yoshikawa, Y. Itoh, T. Nakamura, and H. Utumi, *Physica C* **468**, 1451 (2008).

⁹T. Nakamura, Y. Itoh, M. Yoshioka, N. Sakai, S. Nariki, I. Hirabayashi, and H. Utumi, *TEION KOGAKU* **46**, 139 (2011) (in Japanese).

¹⁰T. Nakamura, J. Uzawa, Y. Itoh, and T. Oka, The 42nd Annual Meeting of the NMR Society of Japan, 2003, p. 326.

¹¹Y. Iwasa, *Physica C* **445–448**, 1088 (2006).

¹²S. B. Kim, R. Takano, T. Nakano, M. Imai, and S. Y. Hahn, *Physica C* **469**, 1811 (2009).

¹³M. Tomita, Y. Fukumoto, K. Suzuki, A. Ishihara, and M. Muralidhar, *J. Appl. Phys.* **109**, 023912 (2011).

¹⁴R. Shigeki and K. Kose, *Proc. Int. Soc. Mag. Reson. Med.* **18**, 1542 (2010).